LIMITS TO THE VELOCITY OF SOLID ARMATURES IN RAILGUNS

G. C. Long and W. F. Weldon

Presented at the
4th Symposium on Electromagnetic
Launch Technology
Austin, Texas
April 12-14, 1988

Publication No. PR-86
Center for Electromechanics
The University of Texas at Austin
Balcones Research Center
EME 1.100, Building 133
Austin, TX 78758-4497
(512)471-4496

Limits to the Velocity of Solid Armatures in Railguns

Glen C. Long
Department of Electrical Engineering
United States Military Academy
West Point, New York
10996

William F. Weldon
Center for Electromechanics
University of Texas at Austin
Austin, Texas
78758

Abstract- The limit to the velocity of a solid armature in a railgun is based upon temperature and the internal forces which surpass the yield strength of the material. A two dimensional finite element model for the magnetic and temperature fields in a railgun is presented for several rail and armatures designs. Copper rails and a molybdenum armature are identified as candidates for future solid armature testing. All simulations are performed for a one-half inch square bore railgun.

INTRODUCTION

There are several railgun applications in which it is desirable to have a solid conducting armature complete the current path between the rails. In order to prevent railgun damage due to ohmic heating and/or internal forces, it is necessary to understand and model the current density distribution within the conducting medium. The mechanical yield strength of the railgun materials is lowered by the increase in temperature which is caused by the electrical current flow(Joule heating), friction, and the contact potential drop. The armature is the critical component in the railgun since it conducts the full system current for the entire length of the rails. Critical temperatures are typically achieved at the rail/armature interface. For the single shot railgun, the rail temperature at the rail/armature interface does not become a problem because the motion of the armature insures that the electrical current always flows through new rail material. Critical rail temperatures may be attained in the rails at the breech end of the railgun.

Joule heating is a volume effect, and the friction/contact potential heating are surface effects at the rail/armature interface. The heat inputs due to friction and the contact potential are not well defined quantities. There has been little research performed to establish the coefficient of friction and the contact potential drop for a sliding interface travelling at a velocity greater than 1 km/sec. Some experiments have established the coefficient of friction in the 0.05-0.3 range and the contact potential drop to be approximately 5 volts per rail. Although friction and the contact potential are important heat sources, most of the armature temperature rise is due to Joule heating. Joule heating is directly related to the square of the current density and inversely related to the electrical conductivity of the material. The Joule heating can be optimized (minimum value) by insuring that a uniform current distribution exists within the armature. A uniform current distribution will also serve to reduce the localized frictional heating and evenly distribute the contact potential heat input across the entire rail/armature interface.

The diffusion of the magnetic field in a railgun is dependent upon two factors; the diffusion time and the velocity skin effect. Each material in a physical system requires a certain amount of time to diffuse or absorb a magnetic field. This diffusion time is directly related to the material magnetic permeability, electrical conductivity, and the length of the diffusion distance. The velocity skin effect is a type of diffusion time phenomena and occurs when there is relative motion between two materials. Figures 1 and 2 demonstrate the diffusion time and velocity skin effects, respectively. A rail/armature cross-section is shown with a rail height of 1cm, armature height of 2cm, and armature width of 1cm. This is a symmetrical problem and only one rail and one-half of the armature are shown in the figures. Copper material properties are used for the simulations. The lines within the rail and the armature indicate the locations of 20%, 40%,60%, and 80% of the total system current with respect to the inside surface of the structure. Figure 1 shows the diffusion pattern for two snapshots in time; t=60 usec and t=∞(a steady state situation) for an armature which is held stationary. The current in the armature for the first case is confined to a much smaller area than the fully diffused second case. Since the Joule heating is directly related to the square of the current density, the initial diffusion time may cause a significant increase in the local armature temperature. This temperature rise may be controlled by using a lower conductivity material(while attempting to keep the same specific heat) or increasing the "ramp up" time of the current input.

The more critical problem for temperature rise in the armature is the velocity skin effect. Figure 2 demonstrates the steady state diffusion patterns for a 0 and 1,000 m/sec armature velocity. Since the current cannot immediately diffuse into the rails, a bunching effect occurs in the armature toward the rear of the rail/armature interface. For the 1,000 m/sec case, the current has diffused into only 14% of the rail on the left side of the drawing. Since the temperature rise is proportional to square of the current density, severe armature deterioration will result from the velocity skin effect.

The velocity skin effect coupled with friction and the contact potential drop causes a limit to the velocity of solid armatures in railguns. Three methods have been developed to force a more uniform current distribution in the armature. These methods consist of using a more resistive armature with a higher melting point, a resistive rail, and a graded resistance armature. Figure 3 depicts the resistive rail and the graded resistance armature. In addition, the effects of the velocity skin phenomena can be lowered by appropriately tailoring the trailing edge of the armature.

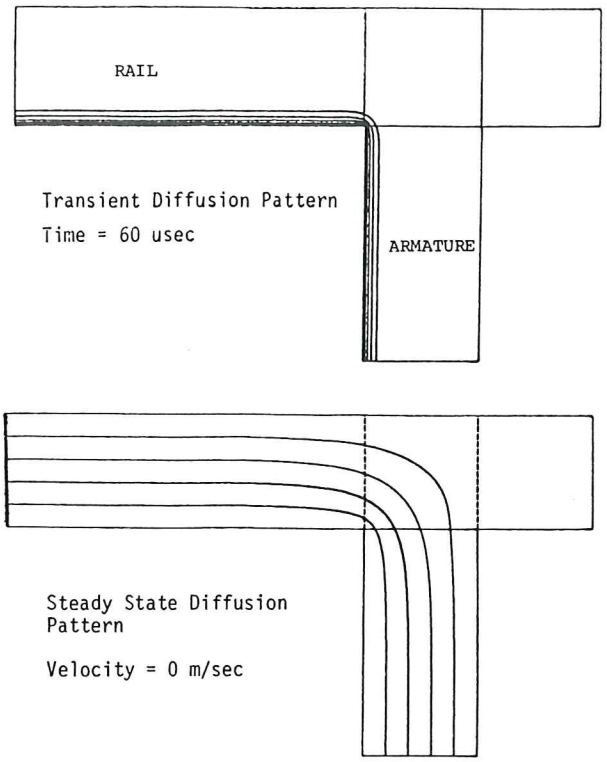

Fig. 1. An example of the initial transient diffusion time.

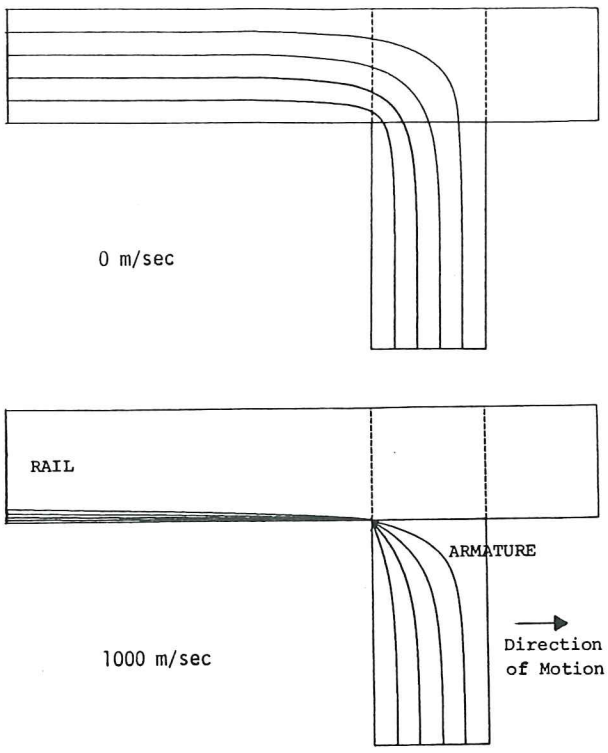

Fig. 2. An example of the velocity skin effect.

The resistive armature decreases the diffusion time of the magnetic field. The diffusion time is inversely proportional to the resistivity of the material. Other factors such as the melting point, density, specific heat, and the thermal conductivity must be considered before using the resistive armature. The resistive rail system is composed of two materials; a highly conductive material layered over a more resistive material. The resistive material faces the armature. An example of two candidate materials for the resistive rail is copper and graphite. The purpose of the highly conductive material is to carry the bulk electrical current through the rails. The resistive layer forces the current diffusion lines to "straighten up" and hence avoid the current bunching effect at the rear of the rail/armature interface. This system may also be viewed in terms of minimum energy concepts. A system minimum energy level will be obtained if the current diffusion lines take the shortest possible path through the resistive rail material. This cannot be obtained if the diffusion lines severely bend toward the rear of the armature.

The graded resistance armature is a layered structure with the materials arranged in decending order of resistivity from the rear of the armature. In the steady state, the electrical current will tend to flow in the most conductive regions of the armature. However, the electrical current must diffuse from the rear toward the front of the armature. The concept of the graded resistance armature is to have the current diffuse through a poor conductor, heat the material, and move toward the next material. Of course, this process occurs as a continuum rather than the discrete nature which may be gleaned from this explanation. The graded resistance armature is a complex design which requires determining the proper material and width for each layer based upon the diffusion time, melting point, and specific heat.

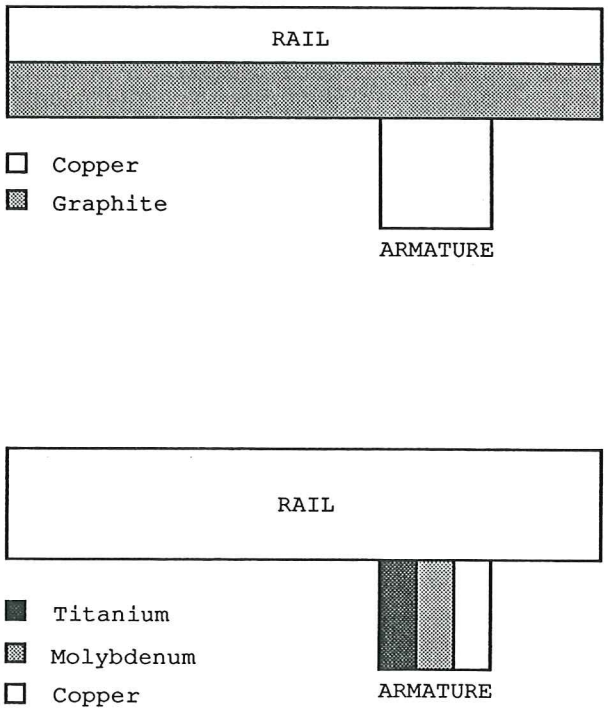

Fig. 3. The resistive rail and the graded resistance armature.

MODELLING

A closed form two dimensional analytic solution for the magnetic field intensity in a railgun has been reported by several researchers[1,2,3]. The distinctions between the various analytical solutions are the result of different simplifying assumptions, aspect of the two dimensions(cross-sectional or along the length of the railgun), and boundary conditions. The analytical solution for the magnetic field intensity is a difficult procedure and practical for only the simplest geometries(homogeneous rectangular rails and armature) and steady state conditions(constant armature velocity). A railgun model with more flexibility than permitted with the analytical solution requires the use of numerical techniques to solve the governing differential equations. The finite difference method has been employed to model the current diffusion process in a cross-sectional area of the rails[4].

The results presented in this paper are derived from a transient finite element electrothermal model for the magnetic and temperature fields. The finite element method offers more flexibility over the finite difference method with regards to analyzing different geometry configurations. The aspect of this analysis is a longitudinal two dimensional area that is centered on the rail/armature interface(See Fig. 4). The equivalent problem of holding the armature stationary and moving the rails backward is modelled by the governing equations and solved using the finite element method. This mathematical technique has the effect of focusing the analysis on the armature since it is the area of most interest for the thermal field calculations.

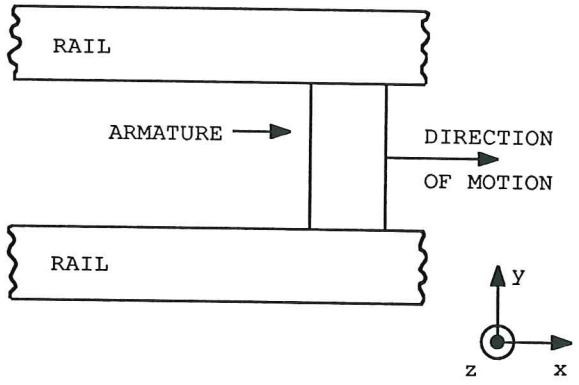

Fig. 4. The two dimension aspect of the finite element analysis.

The solution for the magnetic and temperature fields is based upon the fundamentals of Maxwell's equations and Fourier's law of heat conduction with no apriori assumptions about the current density distribution in the rails or the armature. However, the finite element electrothermal model is a two dimensional representation which assumes that the magnetic field is invariant with respect to the depth of the rails(See Fig. 5). The two dimensional

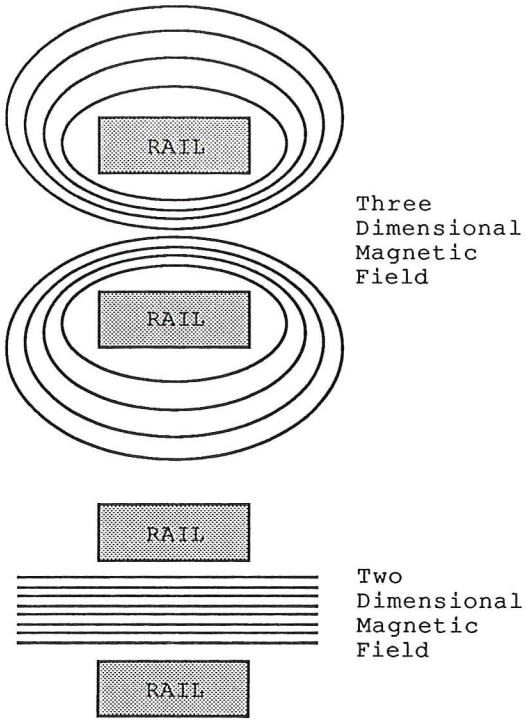

Fig. 5. A comparison between the three dimensional magnetic field and the magnetic field for the two dimensional analysis.

model gives the best approximation of a laboratory railgun near the center region of the rails.

The magnetic field and temperature field spatial variations are calculated using finite element techniques while the time variations are solved using finite differencing methods. A thermal diffusion iteration is performed between each magnetic diffusion iteration. Joule heating information is provided by solving the magnetic diffusion problem. Temperature data for calculating material properties such as the electrical resistivity, thermal conductivity, and specific heat is provided by solving the thermal diffusion problem. User inputs to the finite element model include the geometry of the rails, material properties versus temperature, current input profile versus time, mass of the armature, coefficient of friction data versus speed at the rail/armature interface, and the iteration time step.

The boundary conditions for the magnetic field problem are readily obtained from the two dimensional aspect of the problem. The magnetic field is always a constant value along the inside surface and zero along the outside surface of the rails and armature(See Fig. 4). The constant value of the magnetic field intensity is equal to the rail current divided by the assumed depth of the railgun.

$$H_z = (I/d) \qquad (1)$$

H_z = Magnetic Field Intensity in the z Direction
I = Railgun Current
d = Depth of the Railgun in the z Direction

GOVERNING DIFFERENTIAL EQUATIONS

The governing differential equation for the magnetic field intensity in the railgun is[3];

$$\nabla^2 \mathbf{H} + \sigma\mu[\nabla \times (\mathbf{v} \times \mathbf{H})] = 0 \qquad (2)$$

$\mathbf{H}$ = Magnetic Field Intensity
σ = Electrical Conductivity
μ = Magnetic Permeability
$\mathbf{v}$ = Velocity

The equivalent problem of moving the rails backward and holding the armature stationary will affect the velocity term in equation (2). The two dimensional aspect of the problem requires that the magnetic field exist in only in the (z) direction. Since the magnetic field and the velocity vectors are normal to each other, the diffusion equation for the rail reduces to the following;

$$\frac{\partial^2 H_z}{\partial x^2} + \frac{\partial^2 H_z}{\partial y^2} - v\sigma\mu\frac{\partial H_z}{\partial x} = 0 \qquad (3)$$

The diffusion equation for the armature is;

$$\frac{\partial^2 H_z}{\partial x^2} + \frac{\partial^2 H_z}{\partial y^2} = 0 \qquad (4)$$

The thermal differential equation for the railgun is[4];

$$k\left(\frac{\partial^2 T}{\partial x^2} + \frac{\partial^2 T}{\partial y^2}\right) - cv\frac{\partial T}{\partial x} = c\frac{\partial T}{\partial t} - \frac{J^2}{\sigma} \qquad (5)$$

T = Temperature
k = Thermal Conductivity
c = Specific Heat per Unit Volume
σ = Electrical Conductivity
v = Velocity
J = Electric Current Density
$J = |\nabla \times \mathbf{H}|$

The thermal equation for the armature does not contain the first derivative term since the armature velocity is zero for the equivalent problem. The electrical conductivity(σ), thermal conductivity(k), and the specific heat per unit volume(c) are functions of temperature and the spatial variables (x) and (y). The analysis maintains separate and time changing values of (σ),(k), and (c) for each element in the finite element grid. The magnetic and thermal differential equations are coupled through the $\sigma(x,y,T)$ and $[J(x,y)]^2$ terms, respectively.

SIMULATION RESULTS

Various types of rail and armature designs are simulated to include armatures consisting of different homogeneous materials, the graded resistance armature, and the resistive rail. The analysis includes different solid armature shapes such as the square, curved, chevron, and contact assured designs (See Fig. 6). The contact assured armature

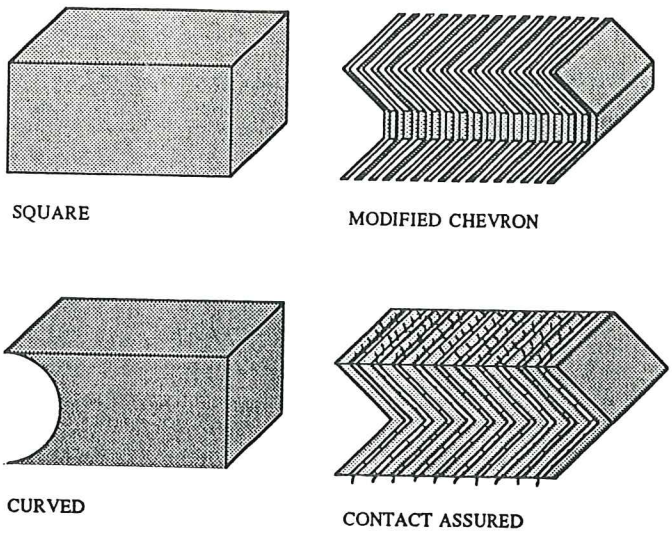

Fig. 6. Various armature designs used for the finite element simulations.

has wire fingers that extend from the chevron and make the electrical contact with the rails. All simulations are performed for a one-half inch square bore railgun.

The analysis output consists of a comparison of armature kinetic energy levels for different railgun designs. Six steady state current levels are analyzed for each case. The current levels include 100 kA, 120 kA, 150 kA, 225 kA, 300 kA, and 400 kA. For all current levels, the input current is allowed to "ramp up" to the steady state level at a rate of 2×10^9 amps/sec(300 kA in 150 μsec). The current per unit depth(z direction) provided by 300 kA in a 1/2" square bore railgun is approximately the same current density required to propel a 1.5 kg launch package in a 9 MJ, 90mm tactical railgun. *The analysis is halted when the temperature in any element of the finite element grid surpasses the melting temperature of its respective material.* This places a rather conservative estimate on the life of the armature. The melting point location usually occurs at the trailing edge of the armature near the rail/armature interface.

Figure 7 demonstrates a comparison between a 1/4", 1/2", and 3/4" long copper square armature. Two factors affecting the kinetic energy levels are evident in the demonstrated results. For current levels greater than 300 kA, the results for each armature are approximately the same and do not depend upon the armature length. This is due to the fact that the current(magnetic field) requires a specified amount of time to diffuse through any material. Since the current is not able to fully diffuse through the armature and reduce the current density, Joule heating becomes a problem at the trailing edge of the material. Hence, each armature begins to melt at approximately the same time. For the lower current levels, the current becomes more evenly distributed throughout the armature. The longer armature has a lower current density, lower Joule heating, and a longer time before melting. The square design is a liability for the armature. Since the current density is equal to the spatial derivative of the magnetic field intensity, $\mathbf{J} = \nabla \times \mathbf{H}$, the trailing corner of the armature experiences

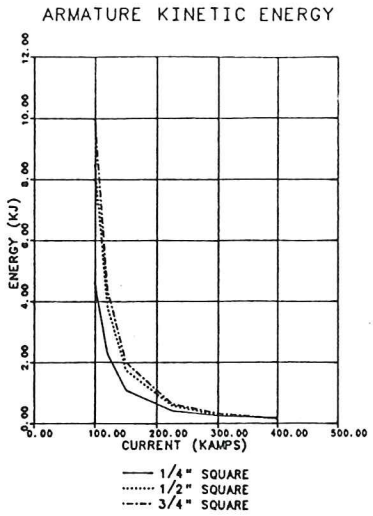

Fig. 7. Comparison of the copper square armatures. The armature lengths are 1/4", 1/2", and 3/4".

significant Joule heating because of the radical change in the geometry from the rail to the armature. The next example demonstrates the benefit of a curved design on the trailing edge of the armature.

Figure 8 presents a comparison between the copper square, curved, and chevron armature designs. The square and chevron designs have a length of 1/2". The curved design has a length of 3/4" at the rail/armature interface and a length of 1/2" along the axis of the railgun. The curved and chevron armature designs have a higher kinetic energy level than the square armature design. This is the result of a less radical geometry change that occurs at the rail/armature interface. The higher performance of the curved armature at the lower current levels can be attributed to its larger mass. The curved armature design contains approximately 25% more mass than the chevron armature design. The increased mass of the curved armature can absorb more Joule heating through the heat capacity of the material.

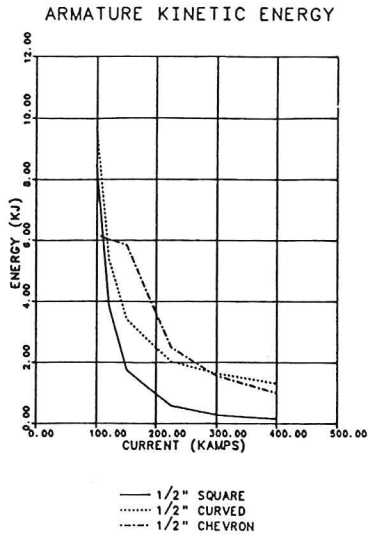

Fig. 8. Comparison of the copper square, curved, and chevron armatures designs.

Figure 9 depicts a comparison between the copper, molybdenum, and aluminum 1/2" long chevron armatures. Molybdenum is a refractory metal that has a melting point of 2,610° C. The results in the figure indicate that molybdenum has a higher performance level than copper or aluminum. For the 300 kA level, the armature kinetic energies for the molybdenum, copper, and aluminum are 12.9 kJ, 1.6 kJ, and 0.5 kJ, respectively. An interesting characteristic of the molybdenum energy plot is the downturn of the energy level for the 100 kA input current. The increased melting time and the lower Joule heating at this current level are not sufficient to correct for the loss of force on the armature due to the lower current. This is an indication that the current distribution attains a fully diffused steady state condition in the 1/2" long molybdenum chevron armature for a current level slightly above 100 kA.

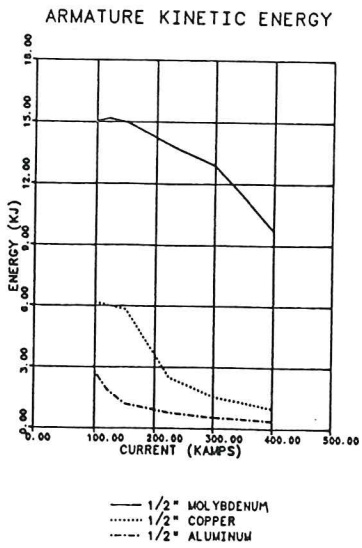

Fig. 9. Comparison of the molybdenum, copper, and aluminum 1/2" long chevron armatures.

The performance of molybdenum may cause the reader to consider other refractory metals for the armature. The refractory metals tend to have higher melting temperatures, higher densities, and moderate resistivities. Unfortunately, the higher melting point and the corresponding lower diffusion time(due to the increased resistivity) is not sufficient to correct for the increased Joule heating and weight of the armature. Figure 10 demonstrates a comparison between the 1/2" long copper square, molybdenum chevron, and tantalum chevron armatures. The melting temperature of tantalum is 2,996° C. The results in the figure indicate a better performance level for molybdenum.

Figure 11 presents the resistive rail design. The resistive rail design is compared with a 1/2" long molybdenum chevron armature on a homogeneous copper rail. The resistive rail consists of a 1/4" layer of molybdenum and a 1/4" layer of copper. The molybdenum is located on the inside surface of the rail. A 1/2" long copper chevron armature and a 1/2" long molybdenum chevron armature are analyzed for the resistive rail. The results of Fig. 11 indicate that the performances of the two modified chevron armatures with a resistive

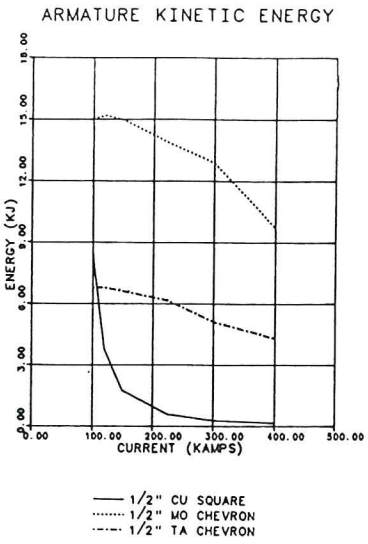

Fig. 10. Comparison of the 1/2" long copper square, molybdenum chevron, and tantalum chevron armature designs.

rail are less than the molybdenum chevron armature with a homogeneous copper rail. The explanation for this phenomena is based upon the increased temperature at the rail/armature interface. The reduction of the velocity skin effect is not sufficient to correct for the increased heating on the rail side of the rail/armature interface. The increased heating and lower thermal conductivity of the resistive rail reduce the armature heat loss through convection and thermal diffusion.

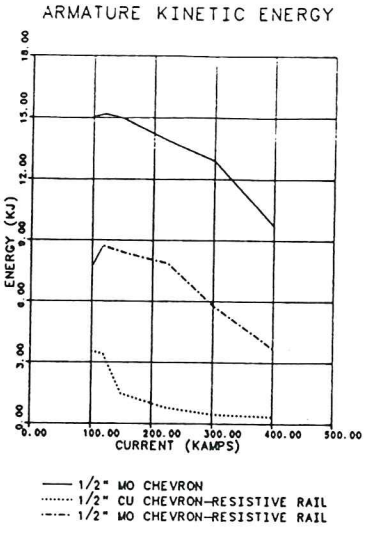

Fig. 11. The effects of the resistive rail compared with the homogeneous copper rail.

Figure 12 depicts a comparison between a molybdenum chevron armature and two graded resistance armatures using a homogeneous copper rail. The graded resistance armatures are constructed from molybdenum-tungsten(50% of the armature length for each material) and titanium-molybdenum-copper(33% of the armature length for each material). The molybdenum armature is shown to have the higher performance at all input current levels.

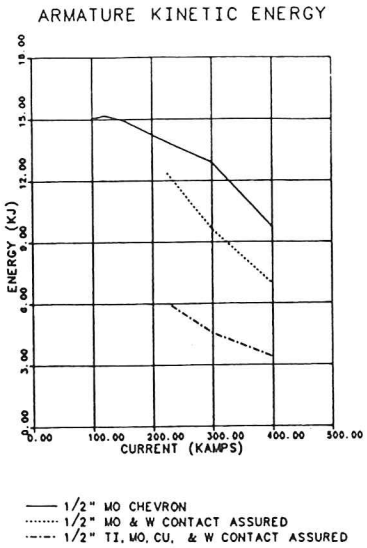

Fig. 12. The effects of the graded resistance armature compared with the molybdenum chevron armature.

CONCLUSIONS

It should be apparent that a numerical technique is the only practical method for solving the set of railgun interdependent governing differential equations. The two dimensional finite element model discussed in this paper indicates that copper rails and a molybdenum chevron armature are a good design combination for the solid armature railgun.

The two dimensional analytic solution, the finite difference model, and the transient finite element analysis are merely intermediate steps toward achieving the goal of a consummate mathematical model for the electromagnetic railgun. This complete model must be a three dimensional analysis that solves the magnetic, temperature, and stress-strain differential equations. This task is probably an engineering problem waiting for the next generation of computer since the two dimensional finite element models for the railgun require considerable computation time on present day supercomputers.

REFERENCES

[1] J.P. Barber, R.A. Marshall, and P. Muttik, "Projectile and Current Behavior in A.N.U. Railgun," 25th Meeting of the Aeroballistics Range Association, October 1984.

[2] F.J. Young and W.F. Hughes, "Rail and Armature Current Distributions in Electromagnetic Launchers," *IEEE Transactions on Magnetics*, Vol. MAG-18, No. 2, January 1982,pp 33-41.

[3] G.C. Long, "Railgun Current Density Distributions," *IEEE Transactions on Magnetics*, Vol. MAG-22, No. 6, November 1986, pp 1597-1602.

[4] J.F. Kerrisk, "Current Diffusion in Railgun Conductors," Los Alamos National Laboratory Report, LA-9401-MS, June 1982.

[5] G.C. Long, "Fundamental Limits to the Velocity of Solid Armatures in Railguns," Ph.D. Dissertation, The University of Texas at Austin, June 1987.